Gas-Phase Vibrational Spectroscopy and Ab Initio Study of Organophosphorous Compounds: Discrimination between Species and Conformers

A. Cuisset,*,† G. Mouret,† O. Pirali,‡,§ P. Roy,‡ F. Cazier,|| H. Nouali,|| and J. Demaison⊥

Laboratoire de Physico-Chimie de l'Atmosphère CNRS UMR 8101, Université du Littoral Côte d'Opale, 189 A Ave. Maurice Schumann, 59140 Dunkerque, France, Ligne AILES (Advanced InfraRed Line Exploited for Spectroscopy), Synchrotron SOLEIL, L'Orme des Merisiers, Saint Aubin, BP 48, 91192 Gif-sur-Yvette, France, Laboratoire de PhotoPhysique Moléculaire, Bâtiment 210, Université Paris-Sud, 91405 Orsay Cedex, Centre Commun de Mesures, Bâtiment MREI1, Université du Littoral Côte d'Opale, 145 Ave. Maurice Schumann, 59140 Dunkerque, France, Laboratoire de Physique des Lasers, Atomes et Molécules, UMR 8523, Bât. P5, Université des Sciences et Technologies de Lille, 59650 Villeneuve d'Ascq, France

Received: May 27, 2008; Revised Manuscript Received: July 21, 2008

Gas phase vibrational spectra of dimethyl methylphosphonate (DMMP), trimethyl phosphate (TMP), and triethyl phosphate (TEP) have been measured using FTIR spectroscopy. For DMMP, TMP, and TEP, most of the infrared active vibrational modes have been observed in the 50−5000 cm^{-1} spectral range, allowing an unambiguous discrimination between the three molecules. The vibrational analysis of the spectra was performed by comparing with MP2 and B3LYP harmonic and anharmonic force field ab initio calculations. The extension to anharmonic calculations provides the best agreement for the mid-infrared and the near-infrared spectra, but they do not improve the harmonic frequency predictions in the far-infrared domain. This part of the vibrational spectra associated with collective and nonlocalized vibrational modes presents the largest frequency differences between the two lowest energy conformers of DMMP and TMP. These two conformers were taken into account in the vibrational assignment of the spectra. Their experimental evidence was obtained by deconvoluting vibrational bands in the mid-infrared and in the far-infrared regions, respectively. For TEP, the conformational landscape appears very complicated at ambient temperature, and a further analysis at low temperature is required to explain the vibrational features of each conformer.

Introduction

Alkyl phosphates [$(RO)_3PO$] and alkyl phosphonates [$(RO)_2P(O)R$] are widely used as model organophosphorus compounds in the analysis of chemical weapon materials, high pathogenic and mutagenic agents, and other environmentally interesting airborne species. Their applications include commercially relevant use as diverse as pesticides, plasticizers, hydraulic fluids, polar organic solvents, or extractant for the nuclear chemical industry. Even for the less volatile, these molecules inevitably impress their environment and strongly react with the most abundant radicals present in the troposphere.[1] Therefore, there is ongoing interest for their detection and quantification in atmospheric conditions. Over several years, different agencies provided support for research evaluating the potential of various chemical and optical techniques to constitute a sensitive and rapid sensor able to identify the phosphoric agent. Dimethyl methylphosphonate [DMMP, $(CH_3O)_2P(O)CH_3$], trimethyl phosphate [TMP, $(CH_3O)_3P(O)$], triethyl phosphate [TEP, $(C_2H_5O)_3P(O)$], and tributyl phosphate [TBP, $(C_4H_9O)_3P(O)$] are among the most studied of the alkyl phosphates and alkyl phosphonates families.

DMMP is a relatively nontoxic agent commonly used in experimental studies as a precursor or stimulant for phosphorus-based nerve agents. Trace gas analysis on DMMP at ppm level of concentration have been performed using an indirect analytical chemistry method[2] or chemisorption on solid substrate,[3] but so far, a direct analysis in an open path with a noninvasive optical method was not available. Nevertheless, numerous fundamental spectroscopic analysis of DMMP was performed, in different energy domains, aiming at providing various properties of this molecule. As example, accurate spectroscopic analysis of DMMP molecules have been performed using Fourier-transform microwave (FTMW) spectroscopy combined with ab initio calculations.[4−6] The assignment of the ground rotational spectrum in the 9.8−21.6 GHz frequency range allowed determination of a large set of rotational and tunnelling parameters.[5] These measurements were performed with a jet-cooled molecular beam, and only the most stable conformer was observed, despite a considerable conformational flexibility for this family of molecules.[4] These studies of DMMP using FTMW spectroscopy instigated similar works on larger alkyl phosphonates, such as diethyl methylphosphonate (DEMP), diethyl ethylphosphonate (DEEP), and diisopropyl methylphosphonate (DIMP).[6] Detection of real chemical-warfare agents has been performed too, using FTMW spectroscopy in surety laboratories. The ground rotational state spectra of different members of the G-series of nerve agents, characterized by a common $R-O-P(O)CH_3F$ molecular backbone, such as sarin ($R = C_3H_7$),[7] soman ($R = C_6H_{13}$),[8] or cyclohexyl sarin (R = cyclohexyl ring),[9] have also been measured. For all these molecules, the comparison between experimental and ab initio parameters such as rotational constants, dipole moment magnitudes, or V_3 barriers of CH_3-P groups provided a partial

* Corresponding author. Tel: 0033(3)28237613. Fax: 0033(3)28658244. E-mail: arnaud.cuisset@univ-littoral.fr.
† Laboratoire de Physico-Chimie de l'Atmosphère CNRS UMR 8101, Université du Littoral Côte d'Opale.
‡ Synchrotron SOLEIL.
§ Université Paris-Sud.
|| Centre Commun de Mesures, Bâtiment MREI1, Université du Littoral Côte d'Opale.
⊥ Université des Sciences et Technologies de Lille.

10.1021/jp804665h CCC: $40.75
Published on Web 09/09/2008

description of the conformational landscape aimed at generating a spectral database of chemical agents and related families of compounds.

Compared with alkyl phosphonates, FTMW spectroscopy studies of alkyl phosphates are not available in the literature. Nevertheless, these molecules present a non-negligible interest in safety programs due to their highly mutagenic and pathogenic activities, which could be explained by their conformational flexibilities.[10] Conformational properties of TMP, TEP, or TBP have been extensively studied using low-resolution vibrational FTIR spectroscopy in gas phase, liquid phase, or rare gas matrices. The conformational landscape remains nevertheless controversial. Infrared and Raman matrix isolation studies coupled with ab initio or semiempirical calculations were the most relevant techniques aimed at describing the conformational landscape.[10−14] The analysis of the vibrational spectrum was limited to the 800−1350 cm^{-1} domain, where the P═O, P−(O−C), and C−C stretching vibrations, the strongest vibrational bands, are observed. In contrast, the far-infrared (FIR) domain remains unexploited.

In the present study, the vibrational spectra of DMMP, TMP, and TEP are measured by FTIR spectroscopy using the room temperature vapor pressure of the compounds, except for TBP, for which the ambient vapor pressure was insufficient for detection. Large sets of infrared active vibrational modes of DMMP, TMP, and TEP have been observed, thanks to the spectral range (50−5000 cm^{-1}) accessible with the FTIR spectrometer. In addition, ab initio calculations have provided a determination of the lowest energy conformations and a simulation of the vibrational spectra. According to these predictions, we demonstrated that mid-infrared and far-infrared domains show some characteristics concerning the discrimination between the compounds and between molecular conformations of each species. The vibrational fingerprints of the two lowest energy conformers of DMMP and TMP are particularly studied. Although experimental evidence of these conformers is accessible in the mid-infrared only for specific modes, such as P═O stretching, most of the low-frequency nonlocalized modes in the far-infrared allow a relevant conformational discrimination.

Experimental Section

Vapor Pressure Measurements. Organophosphorous compounds DMMP, TMP, TEP, and TBP with a stated purity higher than 97% were purchased from Aldrich Chemical Co. and were used without purification. All samples are liquid in standard conditions of temperature and pressure. In this study, saturated vapor pressure at room temperature was injected in a cell dedicated to the spectroscopic studies. Due to the low volatility, especially for the species with the longer carbonyl chains, it was important to have an accurate idea of this physicochemical parameter and its behavior with the temperature. Although, vapor pressure is a key parameter for most environmental fate predictive models, only few data concerning the less volatile system have been reported in the literature.[15] For alkyl phosphates and alkyl phosphonates, several values of vapor pressure at ambient temperature disagree by an order of magnitude or more and except molecules such as TBP,[16] the temperature dependence of the vapor pressure has not been studied. For these reasons, the evolution of the vapor pressures of DMMP, TMP, TEP, and TBP have been measured from room temperature to the boiling point using the static head-space gas-phase chromatography (HS-GC) experimental procedure described previously.[17,18] In brief, 5−10 μL of pure organophosphorous compounds was introduced into 20 mL headspace vials and sealed using silicone septa and aluminum foil. Except for the room temperature measurements, the vials were then thermostated for 30 min. One milliliter of vapor from the above solution was also drawn out from the vial using a gastight syringe and injected directly in the chromatographic column via a transfer line. This sample was then analyzed by a gas chromatograph (Perkin-Elmer Autosystem XL) equipped with a flame-ionization detector using a DB624 column. The GC settings were programmed as following: detector temperature, 280 °C; column temperature, 40 °C during 5 min and heating at 10 °C/min during 20 min. Prior to the HS-GC measurements, a calibration was performed by a direct injection of a known quantity of the products in the column in order to check the linearity and the response factor of the detector. The vapor pressures have been deduced by a comparison with reference values of TBP determined by an empirical law established previously.[16] Figure 1 shows the evolution of equilibrium vapor pressures of DMMP, TMP, TEP, and TBP for eight temperatures from 25 to 180 °C. At 25 °C, the vapor pressures of DMMP, TMP, TEP, and TBP are measured at 130, 110, 40, and 0.1 Pa, respectively. Except for TBP, the temperature dependences of the vapor pressures are quite similar for TMP, TEP, and TBP with a limit value of few kilopascals reached between 120 and 140 °C. For TBP, the variation with the temperature is more important and only a few kilopascals of vapor pressure is observed at 180 °C. For higher temperatures, no measurement was performed because of sample degradation.

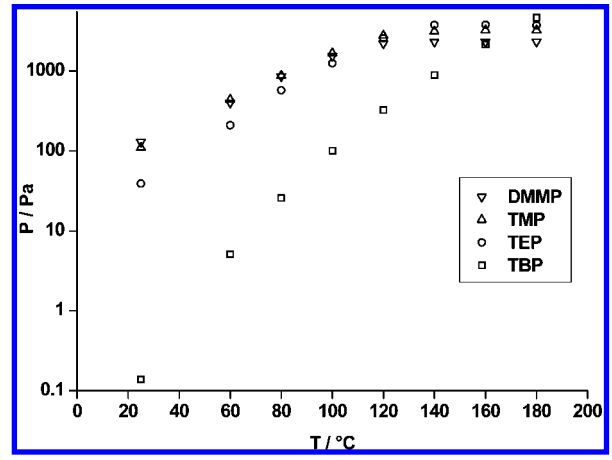

Figure 1. Evolution of the equilibrium vapor pressures of DMMP, TMP, TEP, and TBP from ambient temperature to 180 °C measured by static HS-GC.

Fourier Transform Spectrometer. Gas phase organophosphorous vibrational spectra were recorded in the 50−650 and 600−4000 cm^{-1} frequency regions using the Bruker IFS 125 high-resolution Fourier transform interferometer located on the far-infrared beamline AILES of the synchrotron facility SOLEIL. The MIR (mid-infrared) and the NIR spectra were obtained using a globar source together with a KBr beamsplitter and a MCT detector, while the FIR spectra were recorded by using a mercury lamp as continuum source, together with a composite Mylar beamsplitter and a silicon bolometer cooled at 4 K. All the spectra were recorded with a 0.5 cm^{-1} resolution and result from coadding the Fourier transform of 50 interferograms. In order to limit the absorption of atmospheric compounds, the interferometer was continuously evacuated to 10^{-5} Torr. The interferometer was connected to a multipass cell in which the products at equilibrium vapor pressures at room temperature were introduced. The cell was isolated from the interferometer

using ZnSe or polypropylene windows in the MIR−NIR domains and in the FIR domain, respectively. The optical setup was adjusted to obtain a 24 m optical path length. In the present study, the setup sensitivity was sufficient to detect most of the active infrared modes of DMMP, TMP, and TEP in the 50−4000 cm^{-1} frequency range. For DMMP, TMP, and TEP, spectra were recorded at pressures of about 15 Pa in the FIR and at pressures lower than 5 Pa in the MIR to avoid saturation of the most intense vibrational bands, such as P−O stretching modes at 1100 cm^{-1}.

Computational Methods. All calculations were performed using Gaussian 03[19] associated with its graphical user interface GaussView 03. Structure optimizations and vibrational frequency calculations were done at ab initio second-order perturbed Møller−Plesset (MP2) level of theory[20] and semiempirical density functional theory (DFT) using the Becke[21] three-parameter hybrid exchange functional and the Lee−Yang−Parr correlation functional (B3LYP).[22] The basis sets were chosen considering the necessary compromise between the cost of calculations and the accuracy of the results. MP2 calculations were limited to the 6-311G++(d,p) basis set taking into account the full electronic core correlation. An extension to the 6-311G++(3df,2p) basis set for the phosphorus atom was done in the B3LYP calculations. All the optimizations were performed using the TIGHT and GDIIS convergence criteria, ensuring adequate convergence and the reliability of computed frequencies, especially for low-frequency modes. For the same reasons, the ultrafine grid integral was specified in DFT calculations. Harmonic frequencies calculations were performed with the method and basis set used for the optimization. The absence of imaginary frequencies was checked to ensure that the optimized structure corresponds to a minimum on the potential energy surface. Although the CPU time was 42 and 45 times longer than for the harmonic calculations, it was possible to use B3LYP and MP2 methods for the determination of the anharmonic force field of DMMP and TMP molecules, respectively. For these molecules, the different stable conformations previously determined[4,10] were considered as initial trial geometries. For TEP, the energy surface calculated at the Hartree−Fock/6-31G* level of theory as a function of two different dihedral angles corresponding to different orientations of the ethoxy groups revealed a complex conformational landscape. Because of this high complexity, only the lowest energy conformer was taken into account in the spectroscopic analysis. Optimizations and frequency calculations were performed at the B3LYP/6-31G(d,p) level of theory. Finally, because of the lack of experimental results, no conformational analysis was performed for TBP.

Theoretical and Experimental Results

DMMP and TMP. According to previous studies,[4,10] one expected to observe the spectral fingerprints of the two lowest energy conformations of DMMP and TMP in their vibrational spectra recorded at ambient temperature. The structures optimized at the MP2/6-311++G(d,p) level of theory are shown in Figure 2a,b for DMMP and Figure 2c,d for TMP. Energies, populations, rotational constants, dipole moment components, and optimized values of the O=P−O−C dihedral angles are detailed in Table 1. The molecular parameters obtained with the DFT calculations are also presented in this table.

In this study, the structures predicted by the MP2 method are asymmetric for the two most stable structures of DMMP, called conformer I and conformer II (see Figures 2a,b). In a previous work by Suenram et al.,[4] the MP2 optimization for conformer II converged toward a structure with a symmetry plane defined by the atoms $C_6-P_1=O_3$. In this work, this symmetry plane is predicted only by the B3LYP calculation. These different structures involve discrepancies concerning the energy difference between the two conformers. The B3LYP calculation foresees a population of the conformer I 5 times larger than the population of conformer II. For the MP2 calculation, with a very weak energy difference predicted, the populations of the two conformers are expected to be very close. Nevertheless, the two studies provide an conformer I − conformer II energy difference lower than 350 cm^{-1} (≈1 kcal/mol). Therefore, at 295 K, the population of conformer II cannot be neglected compared to the population of conformer I. A third stable conformation expected with a significantly higher energy (>600 cm^{-1})[4] is not taken into account in this study, as its population at 295 K should represent less than 5% of the complete population of DMMP molecules. Notice that in the previous FTMW study, only conformer I was observed in the 1-K molecular beam.[4]

For TMP, the optimization calculations coherently lead to the low-energy conformational landscape obtained by Reva et al.:[10] Figure 2c,d shows that the lowest energy conformer I has a third-order symmetry axis along the $P_1=O_3$ bond and the second stable conformation is obtained by a displacement of one methyl group from the cis to the trans position. As for DMMP, the energy difference between the conformers I and II of TMP is sufficiently small to expect a significant population of the two conformers in the spectra obtained at ambient temperature. Moreover, in the case of TMP, the symmetries of the conformations imply taking into account the degeneracy of the states when calculating the equilibrium populations. In ref 10, Reva et al. show that with a degeneracy 3 times greater, the lower energy conformer II should be the most abundant, in agreement with the present MP2/6-311++G(d,p) calculation (Table 1). A third stable conformation is also predicted at significantly higher energy (>800 cm^{-1}); therefore, as for DMMP molecules, this conformation was not studied in this work.

The FIR and MIR spectra of DMMP and TMP are shown in Figure 3a,b for DMMP and Figure 3c,d for TMP. Each spectrum is reported with the harmonic frequencies of the two lowest energy conformers obtained using the B3LYP method and allow the assignment of all the observed vibrational bands. Notice, however, that as the experimental spectra show very broad vibrational bands composed of unresolved rotational structures and hot bands involving several quanta of the low frequency modes, all the different modes cannot be easily distinguished. Therefore, a clear discrimination between conformer I and II of DMMP and TMP requires a close examination of the experimental spectra.

TEP and TBP. When methoxy groups are exchanged by ethoxy groups, the motion of the CH_2-CH_3 groups about the O−C axes must be considered in addition to the ethoxy groups about the P−O axes, increasing the number of possible conformations. Therefore, the increase of the number of low-energy conformers for TEP and TBP is directly related to the increasing number of torsional axes.[6] Whereas four and six torsional axes P−O and $O-CH_3$ respectively provided the conformational flexibility of DMMP and TMP, nine and 15 torsional axes including CH_2-CH_3 and CH_2-CH_2 axes have to be taken into account for TEP and TBP, respectively. For alkyl phosphates other than TMP, the theoretical study of the conformational landscape requires one to multiply the number of scans of potential energy surfaces. A possible starting point

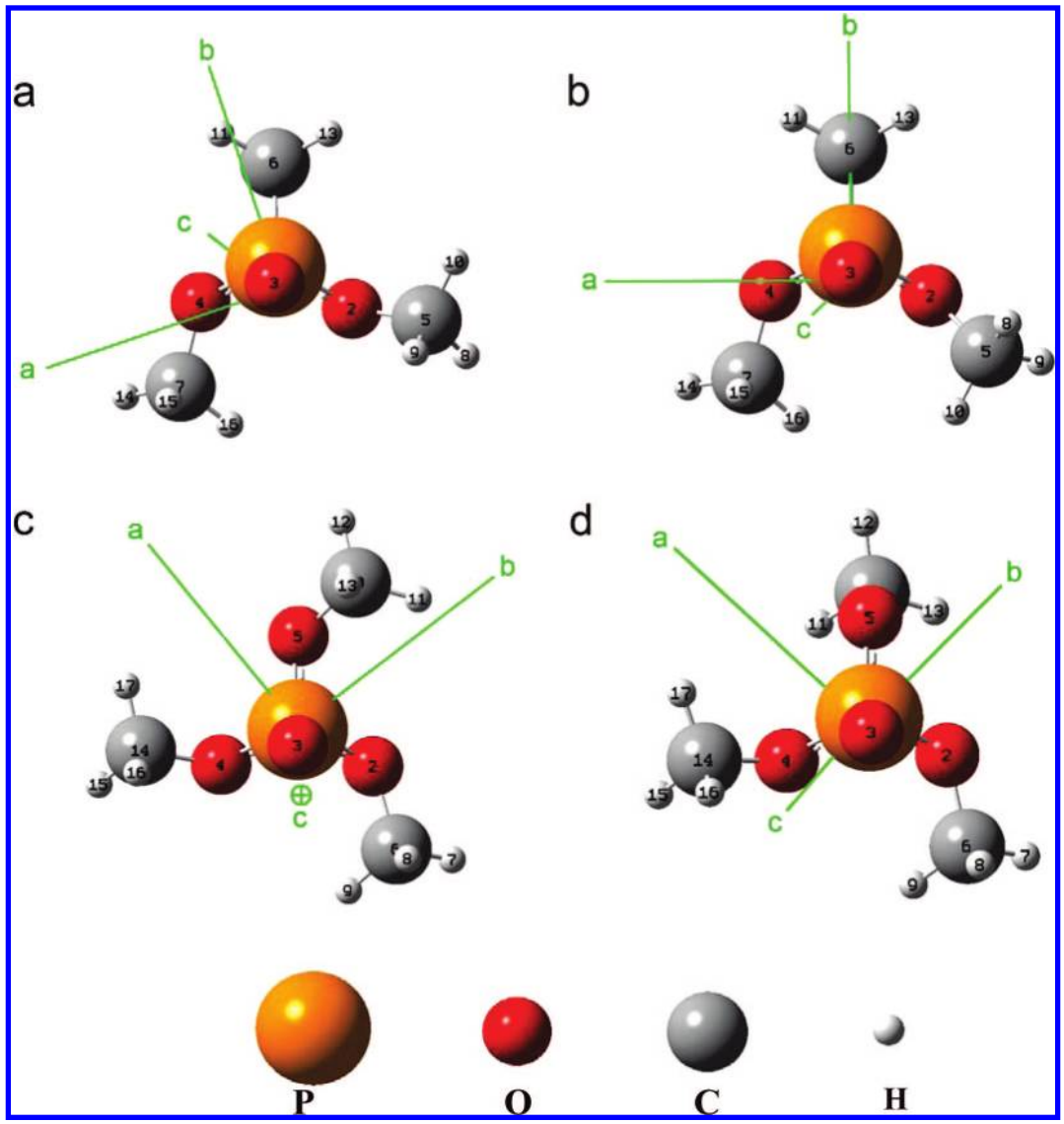

Figure 2. Ab initio structures and principal axes *a*, *b*, and *c* of the two most stable conformers of DMMP and TMP calculated at the MP2/6-311++G(d,p) level of theory. Parts a and b correspond to the conformers I and II of DMMP and parts c and d to the conformers I and II of TMP, respectively. Phosphorus, oxygen, carbon, and hydrogen atoms are represented using 75% of their van der Waals radii.

for this optimization is to localize minima of an energy surface established by varying dihedral angles, implying carbon, oxygen and phosphorus atoms. An example of this surface calculated for TEP at the HF/6-31G* level of theory is shown in the inset (Figure 4). The energy minimum was observed for two dihedral angles O−P−O−C with values between 40° and 50°. These orientations of the ethoxy groups were used as starting geometry for an optimization and a harmonic frequency calculation at the B3LYP/6-31+G(d,p) level of theory. The resulting optimized geometry presented in Figure 4 corresponds to the lowest energy conformer calculated. The gas phase vibrational spectrum of TEP recorded at $T = 300$ K and $P = 10$ Pa is compared with the theoretical harmonic spectrum in Figure 5. Because of the insufficient resolution of the spectrum and the conformational complexity of the molecules, only this conformer was considered in the spectral analysis. The full conformational study in the gas phase of TEP requires exploring a large set of potential surfaces reflecting the large flexibility of the molecules. In a previous study[14] using both semiempirical AM1 computations and matrix isolation spectroscopy, Vidya et al. examined the possible conformations of TEP. In this study, nine conformers were predicted with energy differences lower than 800 cm^{-1}. The calculations suggested that the most stable conformers had C_1 symmetry while higher energy conformers presented C_3 symmetry. In the present B3LYP calculation, the most stable structure is predicted to have C_3 symmetry, as shown in Figure 4.

The sensitivity of the IFS 125 spectrometer was insufficient to detect the 0.2 Pa vapor pressure of TBP at ambient temperature. The observation of the gas phase vibrational spectrum of TBP requires increasing significantly the resulting absorbance of these molecules. Figure 1 suggests that heating the sample at 70 °C should increase the vapor pressure up to 10 Pa, the experimental conditions used for studying TEP. Alternatively, observing the vibrational spectra of TBP at ambient temperature would require a significantly longer absorption path.

Discussion

Observed and Predicted Vibrational Frequencies. For DMMP and TMP, the frequencies predicted by quantum chemistry calculations for the lowest energy conformer allowed a full assignment of the vibrational bands observed in the

TABLE 1: Energies, Populations, Rotational Constants, Dipole Moment Components, and Optimized Values of the O=P−O−C Dihedral Angles for the Two Most Stable Conformers of DMMP and TMP

DMMP											
			rotational constants (MHz)			dipole components (D)			angles[c] (deg)		
	energy (cm^{-1})[a]	population[b] at 295 K (%)	*A*	*B*	*C*	$\|\mu_a\|$	$\|\mu_b\|$	$\|\mu_c\|$	O3=P1−C6	O3=P1−O4−C7	O3=P1−O2−C5
conformer I											
experimental[d]	0		2828.8	1972.4	1614.3	–	–	–	–	–	–
MP2[e]	0	59.6	2748.3	1962.8	1603.2	0.59	0.52	2.08	116.3	−52.2	−29.2
B3LYP[f]	0	84.0	2771.7	1941.7	1584.2	0.44	0.50	2.20	115.9	−47.9	−26.4
conformer II											
MP2[d]	170	43.0	2534	2118	1610	0	1.48	1.64	–	–	–
MP2[g]	78	40.4	2500.6	2150.2	1621.3	0.24	0.93	1.96	118.0	−9.0	51.2
B3LYP	334.7	16.0	2560.2	2083.0	1589.6	0	0.70	2.00	117.9	−27.0	27.2

TMP											
			rotational constants (MHz)			dipole components (D)			angles[c] (deg)		
	energy (cm^{-1})[a]	population[b] at 295 K (%)	*A*	*B*	*C*	$\|\mu_a\|$	$\|\mu_b\|$	$\|\mu_c\|$	O3=P1−O4−C14	O3=P1−O5−C10	O3=P1−O2−C6
conformer I											
MP2	0	42.4	1845.7	1845.7	1193.5	0	0	1.03	46.7	46.7	46.7
B3LYP	0	64.6	1841.2	1841.2	1181.8	0	0	1.00	43.5	43.5	43.5
conformer II											
MP2	159.8	57.6	1873.1	1761.1	1308.2	0.37	0.36	4.24	37.2	177.2	55.3
B3LYP	342.4	35.4	1884.1	1748.6	1282.5	0.45	0.38	3.77	35.1	177.5	50.0

[a] Energies relative to the most stable conformers. The zero-point vibrational contribution is included. [b] The equilibrium populations in percent at 295 K are calculated relatively to the energies of the two most stable conformers. For TMP, degeneracy of the states was taken as 2 and 6 for the conformers I and II, respectively.[10] [c] Angles defined from the atoms labeled in the Figure 2. [d] Experimental data, taken from ref 4, were obtained by FTMW measurements in a molecular jet-cooled beam. [e] MP2 calculations were carried out at 6-311++G(d,p) level of theory. [f] B3LYP calculations of DMMP were carried out at 6-311++G(3df,2pd) level of theory for the phosphorus atom and at 6-311++G(d,p) level of theory for the other atoms. [g] From this work.

infrared spectra, as shown in Figure 3 and as listed in Table 1S of the Supporting Information. Optimum scaling factors, defined by $\lambda = \sum_i^N \nu_i^{exp}\nu_i^{calc}/\sum_i^N(\nu_i^{calc})^2$, are currently established in order to eliminate known systematic errors in calculated frequencies.[23] In this study, the optimum scaling factors λ calculated by summations on all assigned vibrational modes and determined for harmonic B3LYP and MP2 calculations are respectively 0.9676 and 0.9496 for DMMP and 0.9588 and 0.9399 for TMP. These values confirm that, compared with the MP2 theory, the DFT method is better adapted for the calculation of vibrational frequencies.

For the different levels of computation performed on the conformer I of DMMP, Figure 6 compares the relative uncertainties $(\nu_i^{exp} - \nu_i^{calc})/\nu_i^{exp}$ for each vibrational band observed in the 50−3300 cm^{-1} range. It illustrates that, with the combination of harmonic and anharmonic force field calculations, all the experimental frequencies may be predicted with a relative uncertainty lower than 5%. In figure 6, for the modes with $\nu_i^{exp} > 850$ cm^{-1}, the calculated frequencies are ordered according to the inequality $\nu_i^{anharmonic} > \nu_i^{B3LYP} > \nu_i^{MP2}$ and the anharmonic contribution significantly reduces the relative uncertainties. This last observation is not valid for the low-frequency part of the vibrational spectra ($\nu_i^{exp} < 850$ cm^{-1}). To calculate the anharmonic force field, it is assumed that the amplitudes of the vibrations are small and that the harmonic (quadratic) term is the leading term in the series expansion of the potential. Furthermore, the cubic and quartic potential constants are calculated by numerical differentiation. For these reasons, a loss of accuracy is expected in the case of a large amplitude motion (LAM). When the potential function of the LAM is highly harmonic, as in the case of the internal rotation of a methyl group, it seems that the results are still satisfactory, although there are very few studies of this problem.[24] On the other hand, when the potential is anharmonic, as in the case of the inversion motion in acetamide,[25] the method fails to give reasonable results.

With 72 normal modes, the vibrational analysis of TEP is more complex because of the numerous overlaps among vibrational bands, especially in the FIR region (Figure 5). Nevertheless, the harmonic calculation at the B3LYP/6-31+G(d,p) level of theory allowed the assignment of 57 modes with an average uncertainty of 3.13% (see Supporting Information, Table 1S). In spite of the limited basis set used with the DFT calculation, the vibrational assignment of TEP gives an optimum scaling factor equal to 0.9541 close to the TMP value. As for DMMP and TMP, the largest differences between experimental and theoretical frequencies are observed for the modes with $\nu < 200$ cm^{-1}. While several MIR vibrational modes show sharp and intense structures, allowing a high accuracy for the peak finder procedure, the FIR bands appear to be much broader, revealing other transition types and limiting the determination of the experimental positions. Notice that, in the case of TEP, the presence of numerous low-energy conformations limits the vibrational assignment.

Discrimination between Species. In the ongoing search of new optical methods for the detection and the quantification of chemical agents, one of the main figures of merit is the ability to provide an unambiguous spectral fingerprint. In this work, spectral features in the MIR and FIR spectra of DMMP, TMP, and TEP allow one to efficiently discriminate among these molecules.

In the MIR region, the band ν_{17} of DMMP observed at 919.2 cm^{-1} (Supporting Information, Table 1S) and assigned to a rocking motion of the methyl group of the P−CH_3 group is

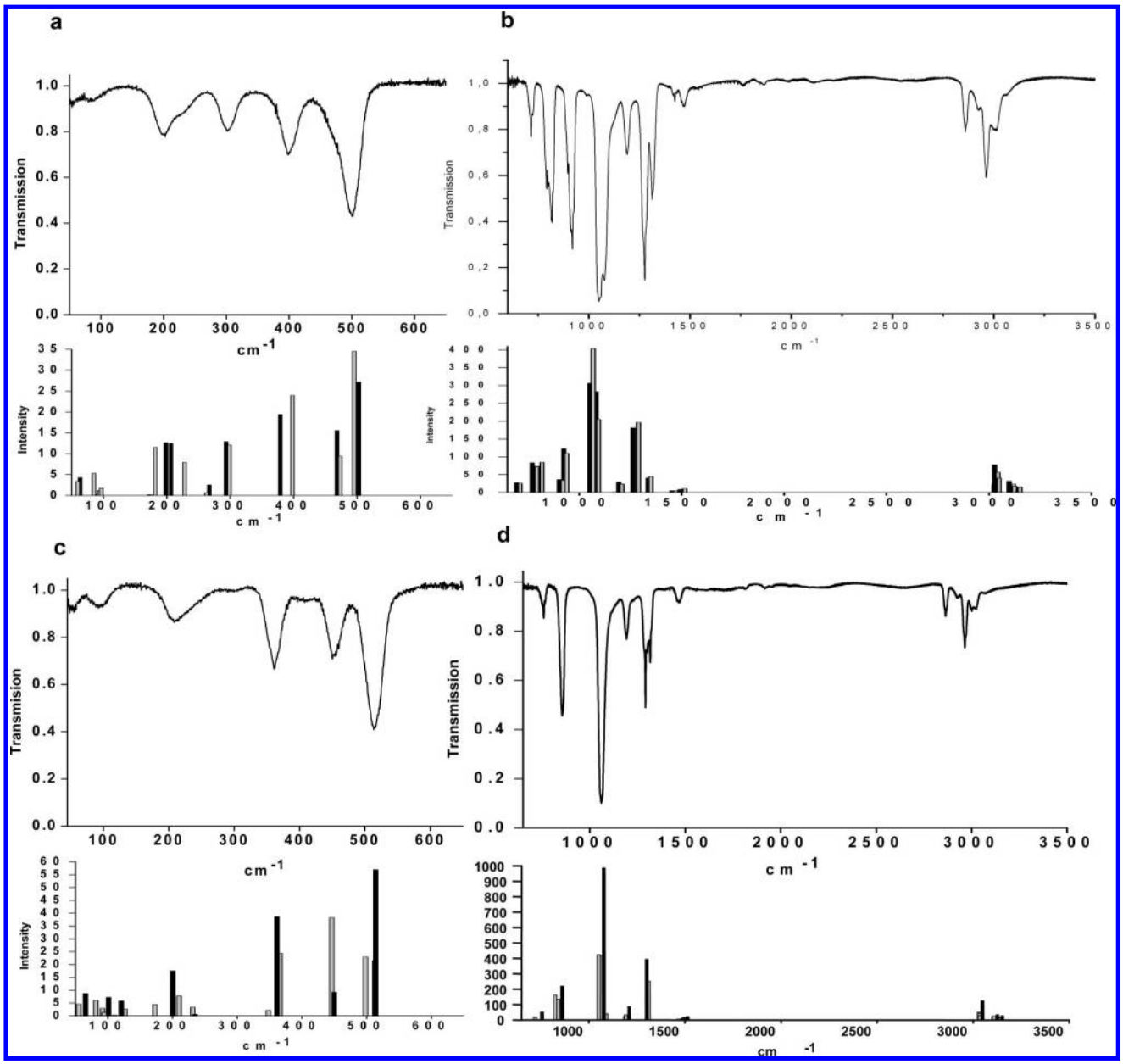

Figure 3. Gas-phase Fourier transform spectra of DMMP (a and b) and TMP (c and d) compared with harmonic B3LYP calculations of the two lowest energy conformers I (light gray) and II (black). FIR spectra (a and c) and MIR−NIR spectra (b and d) were respectively recorded at pressures of 10 and 3 Pa. Theoretical intensities are given in km mol^{-1} per molecule. For the doubly degenerated vibration of conformer I of TMP, intensities are summed.

absent from the spectrum of TMP. The discrimination in the MIR between alkyl phosphates and alkyl phosphonates DMMP and TMP requires comparing the vibrations involving the methyl groups to the vibrations involving the methoxy groups. In the same spectral region, TMP and TEP may be distinguished thanks to the most intense bands of their spectra. For TMP, this band is centered at 1060.2 cm^{-1} and is assigned to the ν_{18-19} O−P−O asymmetric stretching modes. Whereas, for TEP, the equivalent ν_{28-29} mode is centered at 972.5 cm^{-1} and another stronger vibrational band assigned to the ν_{30-31} C−C−O asymmetric stretching of the ethoxy groups is observed at 1050.1 cm^{-1}.

From the FIR spectra, the discrimination between the three species may be performed by considering the frequency shift of the low-frequency vibrations (Figures 3 and 6). For example, a blue-shift is observed with the increase of the size of the molecule for the vibrational bands of DMMP, TMP, and TEP associated with the ν_{10}, ν_{12}, and ν_{18} modes and centered at 398.7, 450.1, and 469.3 cm^{-1}, respectively. The same blue-shift is evidenced for bands ν_{12}, ν_{13-14}, and ν_{19-20} of DMMP, TMP, and TEP centered respectively at 500.4, 513.5, and 538.0 cm^{-1}. All these bands are associated with collective and nonlocalized motions originating from in-plane and out-of-plane O−P−O bending, which seem very sensitive to the modifications of the chemical surroundings. It is plausible that those modes are sensitive to steric effects and the vibrations that correspond to internal rotations are hindered by the presence of the long carbon chains.

Discrimination between Conformers. The calculations performed in this work as well as the numerous previous studies highlighted the large conformational flexibility of organophosphorous compounds such as DMMP, TMP, and TEP. Therefore, it is worthwhile to evaluate the abilities of FTIR spectroscopy combined with quantum chemical calculations to discriminate the spectral fingerprints of each

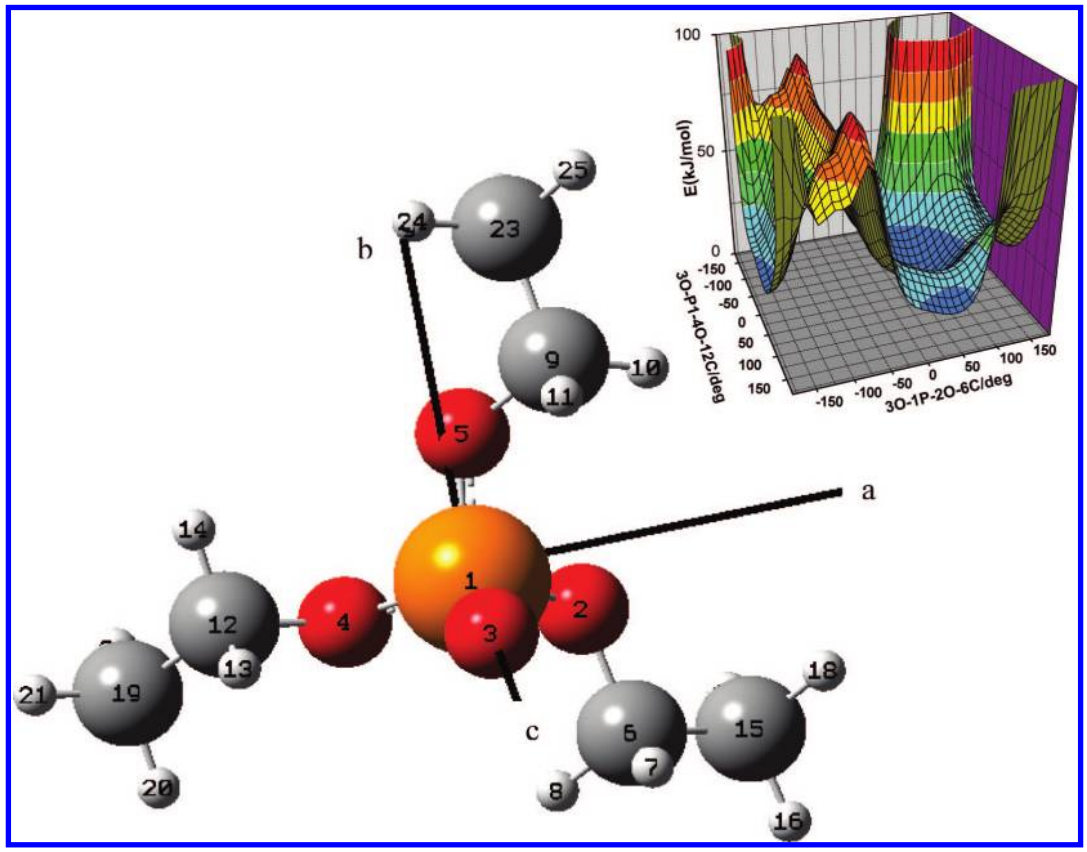

Figure 4. Ab initio structure and principal axes *a*, *b*, and *c* of the lowest energy conformer of TEP calculated at the B3LYP/6-31+G(d,p) level of theory. Inset: Energy surface calculated at the HF/6-31G* level of theory; the global minimum corresponds to the starting geometry for the B3LYP calculation.

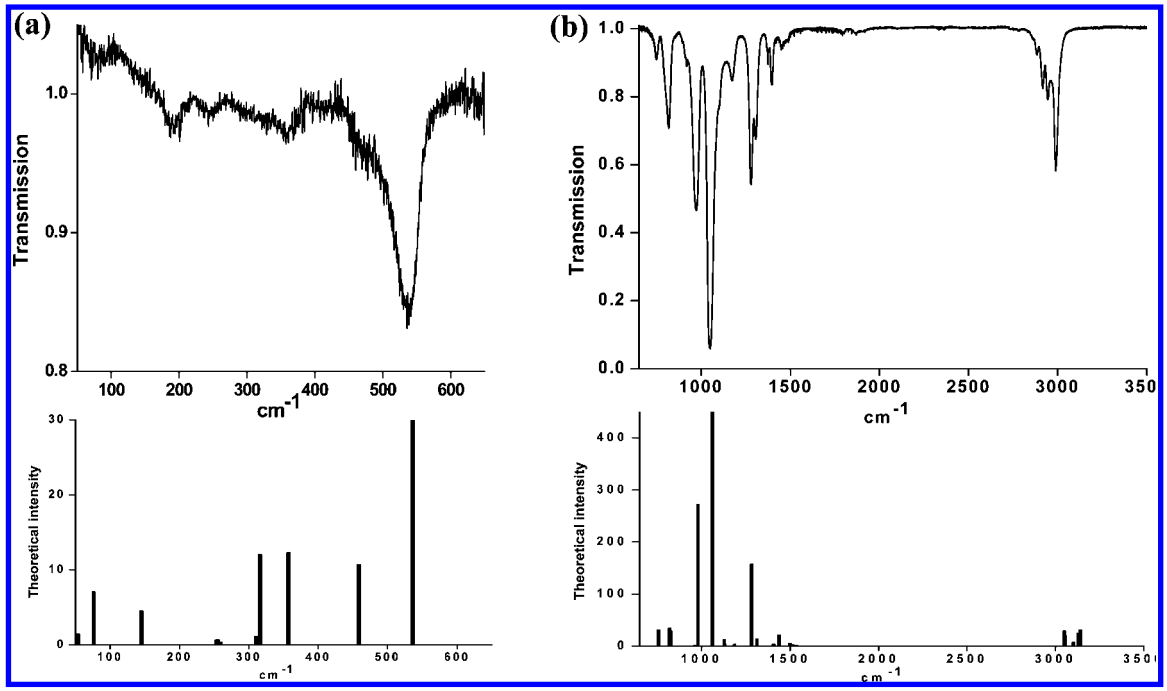

Figure 5. Gas-phase Fourier transform FIR and MIR spectra of TEP (a and b) compared with the theoretical spectra of the lowest energy conformer calculated at the B3LYP/6-31G(d,p) level of theory. FIR and MIR experimental spectra were respectively recorded at pressures of 9 and 3 Pa.

conformer. For TEP, the experimental resolution was insufficient to discriminate the spectral contributions of individual molecular conformations. For this reason, only TMP and DMMP conformational discrimination will be discussed in the following section.

At first, one needs to select the most adapted frequency regions for an unambiguous conformational discrimination. To this aim, Figure 7 presents for each calculated vibrational mode of DMMP and TMP the difference between the harmonic frequencies of the conformers I (CI) and II (CII): $\Delta\nu_{CI-CII} =$

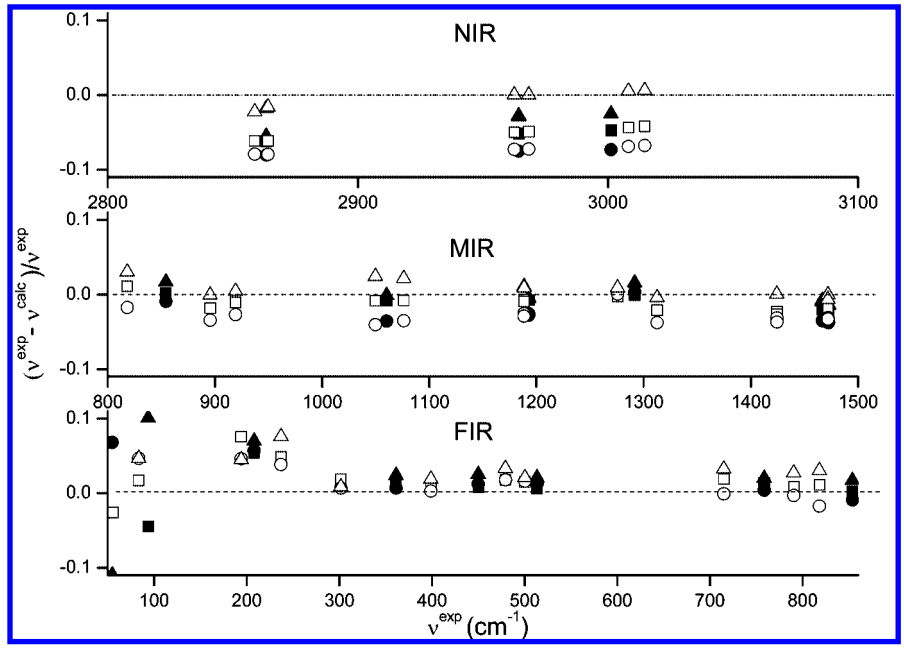

Figure 6. Calculated frequencies of the different vibrations of the conformers I of DMMP (white) and TMP (black) compared to experimental measured frequencies. Relative uncertainties for three different levels of theory are plotted as a function of the frequency of the mode. Circles and squares are associated with the harmonic MP2 and B3LYP calculations. Triangles correspond to the anharmonic field calculations.

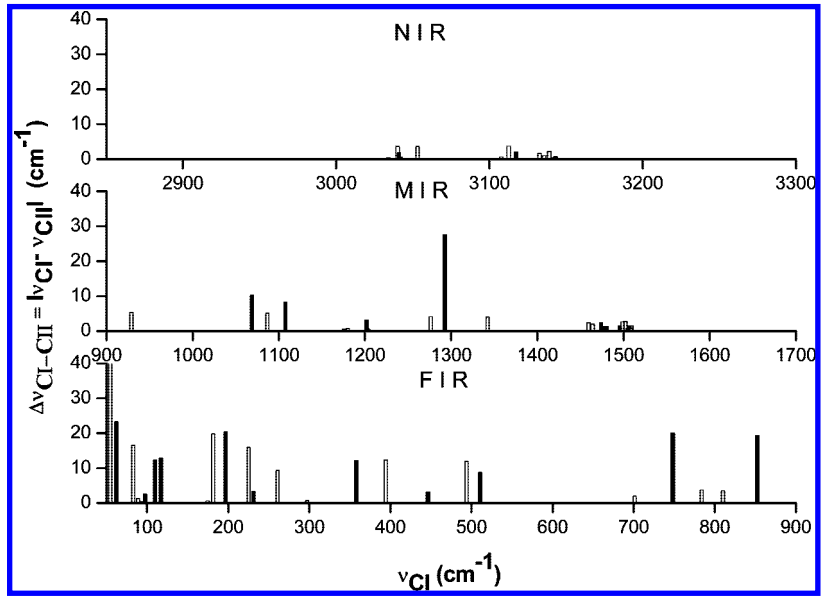

Figure 7. Harmonic frequency differences between the two lowest energy conformers I and II of DMMP and TMP for each vibrational mode in the 50−3300 cm^{-1} spectral domain. Frequencies of DMMP (white) and TMP (black) have been calculated with the B3LYP method.

$|\nu_{CI} - \nu_{CII}|$ calculated with the B3LYP method. The results are presented in Figure 7 according to three spectral domains, FIR, MIR and NIR regions, covering respectively the 50−900, 900−1700, and the 2850−3300 cm^{-1} frequency range. The average values of $\Delta\nu_{CI-CII}$ evaluated in the three domains are 8.6 (10.3) cm^{-1}, 2.0 (3.7) cm^{-1}, and 1.6 (0.7) cm^{-1}, respectively obtained for DMMP (TMP). As shown in Figure 7, for both DMMP and TMP, the FIR region presents the largest energy differences between conformers. In contrast to localized stretching C−H modes in the NIR domain, the nonlocalized and collective low-frequency modes are very sensitive to the conformation of the molecule. This may explains resorting to FIR and THz spectroscopy to study the conformational flexibility of biomolecules.[26,27] It should be noted, however, as illustrated in Figure 7, that the MIR region shows a specific frequency calculated for the TMP conformer I at 1292.75 cm^{-1} with a large value of $\Delta\nu_{CI-CII}$ close to 30 cm^{-1}. This frequency is associated with the mode ν_{27} of TMP corresponding to the P═O stretching of the TMP molecules. The comparison between the two conformations (Figure 2) shows three intramolecular hydrogen bonding between the methyl hydrogen and the phosphoryl oxygen for the conformer I and two for the conformer II. These intramolecular hydrogen bonding probably leads to a lowering of the P═O stretching frequency and explains why the ν_{27} mode is particularly sensitive to the global orientation of the methoxy groups.[11]

Even though theoretical calculations predict several modes as good candidates for the conformational discrimination of DMMP and TMP, the experimental evidence of individual spectral fingerprints of these conformers remains challenging because of the strong overlapping between the vibrational bands and the limited frequency resolution. In Figure 8, the confor-

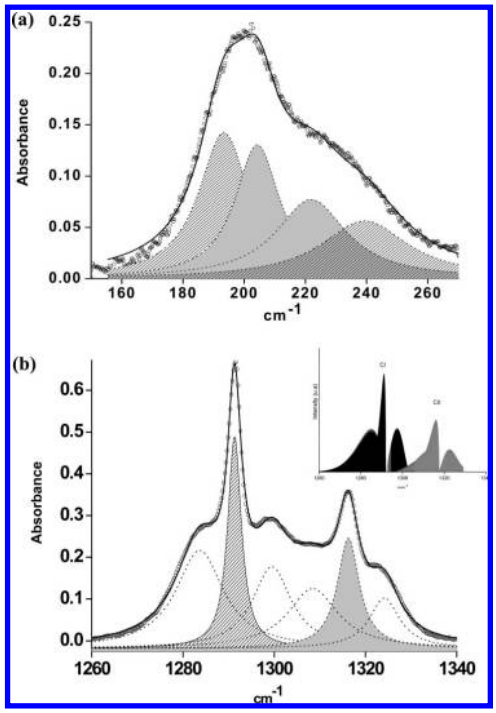

Figure 8. Experimental evidence of the two Conformers I and II of DMMP and TMP in the FIR and in the MIR domain, respectively. (a) Four Lorentzian bands are used in order to reproduce the bands ν_6 and ν_7 of the conformers I (hatched bands) and II (filled bands) of DMMP. (b) The hatched band and the filled band are associated with the Q branch of the mode ν_{27} of the conformers I and II of TMP, respectively. The four other bands were required in order to reproduce the P and R branches of each conformer. (Inset to b) Simulation of the rotational pattern using a simple asymmetric rotor predictive model[28] for the two conformers.

mational analysis of the vibrational bands observed in the 150−270 cm^{-1} and 1250−1350 cm^{-1} frequency ranges, respectively, for DMMP and TMP are presented. These bands were chosen because of the large difference $\Delta\nu_{CI-CII}$ as reported in Figure 7. For DMMP (Figure 8a), the measured absorbance is rather weak and broadened. For TMP (Figure 8b), a strong intensity multiplet structure with two thin peaks is observed. Thanks to the comparison with theoretical calculations, it is possible to identify the individual contributions of each conformer I and II to these structures.

For DMMP, the band was fitted using four Lorentzian contributions for which the frequency differences and the relative intensities were chosen using the harmonic DFT calculations of modes ν_6 and ν_7 of conformers I and II. The linewidths of each component were arbitrary fitted. The fitting with these four Lorentzians allowed a good agreement with the experimental structure. Notice finally that compared to the previous work of Suenram et al.,[4] where conformer II was not observed due to collisional cooling in the molecular beam, in this work at room temperature, the FIR gas-phase spectra evidence the influence of conformer II on the vibrational fingerprint. The relative intensities suggest that the populations of the two conformers are very close, in agreement with the energies determined with the MP2 calculations (Table 1).

For TMP, a similar conformational analysis may be done with the structure of the band located in the 160−280 cm^{-1} region, where the ν_7 and ν_8 modes of conformers I and II are predicted. These two conformers are also easily distinguished in the band located in the 1260−1340 cm^{-1} frequency region associated with the mode ν_{27} corresponding to the P═O stretching of TMP, for which the largest difference $\Delta\nu_{CI-CII}$ is predicted in the MIR (see Figure 7). Figure 2 shows the coincidence between the P═O double bond and the *c*-axis of the TMP molecule. Therefore, the mode ν_{27} is a strong c-type mode and the multiplet structure observed corresponds to the overlapping of the c-type bands of each conformer. In Figure 8b, the two thin peaks centered at 1291.2 and 1316.2 cm^{-1} are assigned to the Q branches of the mode ν_{27} of conformers I and II, respectively. The Lorentzian fit in Figure 8b shows twice the intensity for conformer I compared to conformer II. This observation agrees with the populations of the two conformers predicted by the MP2 energy calculations (Table 1) and the doubly degenerated vibration of conformer I of TMP. As for DMMP, the relative intensities between the two Q branches confirm that the MP2 calculation yielded more reliable results for the relative energies. P and R branches are also observed for both conformers and were fitted using four Lorentzians. The rotational constants *A*, *B*, and *C* of the ground and the ν_{27} states predicted by the anharmonic field calculations have been used in a simple asymmetric rotor predictive model[28] to simulate the rotational pattern of the ν_{27} bands of the two conformers. The two simulated c-type bands, shown in the inset of Figure 8b, closely reproduce the fitted multiplet structure. This band has been previously described by Reva et al.[10] in the vibrational spectra of TMP obtained in xenon matrix. In this work, a shoulder located between the two main lines was observed and explained by the significant contribution of a third conformation, although ab initio calculations predicted a significantly higher energy for this conformer (>600 cm^{-1}) and therefore a very unlikely observation. In this work, the rotational structure of the two main conformers tends to blend this part of the spectrum, and the signature of a third conformer could not be confirmed.

Conclusions

Using Fourier-transform infrared spectroscopy, the gas-phase spectra of DMMP, TMP, and TEP have been measured, analyzed, and compared. The quasicomplete set of the infrared active vibrational modes of these molecules was assigned thanks to the large spectral range accessible (50−5000 cm^{-1}). The spectroscopic analysis combined with quantum chemical calculations allowed us to partially describe the conformational landscape of these molecules. The ability of gas-phase vibrational spectroscopy to discriminate the molecules and their conformers was discussed. For DMMP and TMP, the vibrational fingerprints of the two lowest energy conformers may be discriminated, thanks to either specific high intensity c-type modes in the MIR region or to the collective low-frequency vibrations observed below 850 cm^{-1}. Compared to MIR, the vibrational assignment in the FIR region does not require taking into account the anharmonicity of the modes and is free from the confusing extra structures such as combinations bands or overtones directly observable in the 1500−2500 cm^{-1} spectral region (Figures 3b,d and 5d). The harmonic frequency calculations showed that the largest frequency differences for the two lowest energy conformers of DMMP and TMP are predicted for the lowest energy vibrational modes below 80 cm^{-1}. These low-frequency vibrations, observed at the limit of the tunability of the FTIR spectrometer, may be reached with THz optoelectronic radiations. Recent studies underlined the potential of optoelectronic THz techniques such as THz time-domain spectroscopy[29] or continuous-wave THz spectroscopy[30] for their abilities to detect and quantify chemical agents. Photomixing THz sources allows measuring pure rotational transitions of light polar molecules at frequencies up to 3 THz (≈100 cm^{-1}) with

a resolution close to 3 MHz (≈0.0001 cm^{-1}).[31] Using these sources, it should be possible to resolve and to discriminate the rotational structures of each conformer observed in the lowest frequency part of the vibrational spectra. Nevertheless, because of the weak intensity of the low-frequency modes, the success of the experience requires a significant improvement of the sensitivity of the THz spectrometers, which remains the main weakness of the method.[32]

In the future, the exceptional properties of the infrared beam line of the synchrotron radiation,[33] in particular its high brilliance allowing longer path length in the gas cell, will be exploited for the study of the less volatile molecules, such as TEP and TBP. Finally, the increase of observable conformations suggests studying these highly flexible molecules in a jet-cooled supersonic expansion in order to simplify the conformational landscape and, therefore, the assignment of the vibrational spectra.

Acknowledgment. This work was supported by the Délégation Générale pour l'Armement (DGA) (projet de Recherche Exploratoire et Innovation no. 06.34.037). D. Dewaele, S. Eliet, and L. Vieren are thanked for their help in the headspace measurements. The Laboratoire de Physico-Chimie de l'Atmosphère participates in the "Centre d'Etudes et de Recherches Lasers et Applications" (CERLA) and "Institut de Recherche en ENvironnement Industriel" (IRENI).

Supporting Information Available: Experimental and calculated vibrational frequencies and intensities for the lowest energy conformer of DMMP, TMP, and TEP are collected (Table 1S). This material is available free of charge via the Internet at http://pubs.acs.org.

References and Notes

(1) Aschmann, S. M.; Tuazon, E. C.; Atkinson, R. *J. Phys. Chem. A* **2005**, *109*, 11828.

(2) Tevault, D. E.; Pellenbarg, R. E. *Sci. Total Environ.* **1988**, *73*, 65.

(3) Ewing, K. J.; Dagenais, D. M.; Bucholtz, F.; Aggarwal, I. D. *Appl. Spectrosc.* **1996**, *50*, 5.

(4) Suenram, R. D.; Lovas, F. J.; Plusquellic, D. F.; Lesarri, A.; Kawashima, Y.; Jensen, J. O.; Samuels, A. C. *J. Mol. Spectrosc.* **2002**, *211*, 110.

(5) Ohashi, N.; Pyka, J.; Golubiatnikov, G. Yu; Hougen, J. T.; Suenram, R. D.; Lovas, F. J.; Lessari, A.; Kawashima, Y. *J. Mol. Spectrosc.* **2003**, *218*, 114.

(6) DaBell, R. S.; Suenram, R. D.; Lavrich, R. J.; Lochner, J. M.; Ellzy, M. W.; Sumpter, K.; Jensen, J. O.; Samuels, A. C. *J. Mol. Spectrosc.* **2004**, *228*, 230.

(7) Walker, A. R. H.; Suenram, R. D.; Samuels, A.; Jensen, J.; Ellzy, M. W.; Lochner, J. M.; Zeroka, D. *J. Mol. Spectrosc.* **2001**, *207*, 77.

(8) Suenram, R. D.; DaBell, R. S.; Walker, A. R. H.; Lavrich, R. J.; Plusquellic, D. F.; Ellzy, M. W.; Lochner, J. M.; Cash, L.; Jensen, J. O.; Samuels, A. C. *J. Mol. Spectrosc.* **2004**, *224*, 176.

(9) Suenram, R. D.; DaBell, R. S.; Plusquellic, D. F.; Ellzy, M. W.; Lochner, J. M.; Jensen, J. O.; Samuels, A. C. *J. Mol. Spectrosc.* **2005**, *231*, 28.

(10) Reva, I.; Simao, A.; Fausto, R. *Chem. Phys. Lett.* **2005**, *406*, 126.

(11) George, L.; Sankaran, K.; Viswanathan, K. S.; Mathews, C. K. *Appl. Spectrosc.* **1994**, *48*, 7.

(12) Sablinskas, V.; Horn, A.; Klaeboe, P. *J. Mol. Struct.* **1995**, *349*, 157.

(13) Streck, R.; Barnes, A. J.; Herrebout, W. A.; van der Veken, B. J. *J. Mol. Struct.* **1996**, *376*, 277.

(14) Vidya, V.; Sankaran, K.; Sundarajan, K.; Viswanathan, K. S. *J. Mol. Struct.* **1999**, *476*, 97.

(15) Kim, Y.; Woodrow, J. E.; Seiber, J. N. *J. Chromatogr.* **1984**, *314*, 37.

(16) Khumar, S.; Koganti, S. B. *Nucl. Technol.* **1999**, *126*, 237.

(17) Kolb, B.; Ettre L. S. *Static Headspace-Gas Chromatography Theory and Practice*; Wiley-VCH, New York, 1997.

(18) Blach, P.; Fourmentin, S.; Landy, D.; Cazier, F.; Surpateanu, G. *Chemosphere* **2008**, *70*, 374.

(19) Frisch, M. J. ; Trucks, G. W.; Schlegel, H. B.; Scuseria, G. E.; Robb, M. A.; Cheeseman, J. R.; Montgomery, J. A., Jr.; Vreven, T.; Kudin, K. N.; Burant, J. C.; Millam, J. M.; Iyengar, S. S.; Tomasi, J.; Barone, V.; Mennucci, B.; Cossi, M.; Scalmani, G.; Rega, N.; Petersson, G. A.; Nakatsuji, H.; Hada, M.; Ehara, M.; Toyota, K.; Fukuda, R.; Hasegawa, J.; Ishida, M.; Nakajima, T.; Honda, Y.; Kitao, O.; Nakai, H.; Klene, M.; Li, X.; Knox, J. E.; Hratchian, H. P.; Cross, J. B.; Adamo, C.; Jaramillo, J.; Gomperts, R.; Stratmann, R. E.; Yazyev, O.; Austin, A. J.; Cammi, R.; Pomelli, C.; Ochterski, J. W.; Ayala, P. Y.; Morokuma, K.; Voth, G. A.; Salvador, P.; Dannenberg, J. J.; Zakrzewski, V. G.; Dapprich, S.; Daniels, A. D.; Strain, M. C.; Farkas, O.; Malick, D. K.; Rabuck, A. D.; Raghavachari, K.; Foresman, J. B.; Ortiz, J. V.; Cui, Q.; Baboul, A. G.; Clifford, S.; Cioslowski, J.; Stefanov, B. B.; Liu, G.; Liashenko, A.; Piskorz, P.; Komaromi, I.; Martin, R. L.; Fox, D. J.; Keith, T.; Al-Laham, M. A.; Peng, C. Y.; Nanayakkara, A.; Challacombe, M.; Gill, P. M. W.; Johnson, B.; Chen, W.; Wong, M. W.; Gonzalez, C.; Pople, J. A. *Gaussian 03, Revision B.04*; Gaussian Inc.: Pittsburgh, PA, 2003.

(20) Møller, C.; Plesset, M. S. *Phys. Rev.* **1934**, *46*, 618.

(21) Becke, A. D. *J. Chem. Phys.* **1993**, *98*, 5648.

(22) Lee, C. T.; Yang, W. T.; Parr, R. G. *Phys. Rev. B* **1988**, *37*, 785.

(23) Wong, M. W. *Chem. Phys. Lett.* **1996**, *256*, 391.

(24) Lovas, F. J.; Groner, P. *J. Mol. Spectrosc.* **2007**, *236*, 173.

(25) Demaison, J.; Császár, A. G.; Kleiner, I.; Møllendal, H. *J. Phys. Chem. A* **2007**, *111*, 2574.

(26) Aviles-Moreno, J. R.; Demaison, J.; Huet, T. R. *J. Am. Chem. Soc.* **2006**, *128*, 10467.

(27) Siegrist, K.; Bucher, C. R.; Mandelbaum, I.; Hight Walker, A. R.; Balu, R.; Gregurick, S. K.; Plusquellic, D. F. *J. Am. Chem. Soc.* **2006**, *128*, 5764.

(28) Pickett, H. M. *J. Mol. Spectrosc.* **1991**, *148*, 371.

(29) Choi, M. K.; Betterman, A. D.; van der Weide, D. W. *Proc. SPIE* **2004**, *5268*, 27.

(30) Podobedov, V. B.; Lavrich, R.; Korter, T. M.; Fraser, G. T.; Plusquellic D. F. NIST Internal Report 2004; p 7134.

(31) Mouret, G.; Matton, S.; Bocquet, R.; Hindle, F.; Peytavit, E.; Lampin, J. F.; Lippens, D. *Appl. Phys. B: Laser Opt.* **2004**, *79*, 725.

(32) Bigourd, D.; Cuisset, A.; Hindle, F.; Matton, S.; Bocquet, R.; Mouret, G.; Cazier, F.; Dewaele, D.; Nouali, H. *Appl. Phys. B: Laser Opt.* **2007**, *86*, 579.

(33) Roy, P.; Rouzières, M.; Qi, Z.; Chubar, O. *Infrared Phys. Technol.* **2006**, *49*, 139.

JP804665H